Polarization measurement errors analysis on fully-automatic polarimetry

Miao Ren, Dongkai Du, Jin Zhang, Haozhe Zhang, Feiya Ma, Xiangyu Zhang, Yanbei Hao, Jian Liang, Xinying Zhao, Liyong Ren*
School of Physics and Information Technology, Shaanxi Normal University, Xi'an 710119, China
*Corresponding author e-mail: renliy@snnu.edu.cn

ABSTRACT

Polarization is a basic and important parameter of light, and polarized light has great applications in optical communications, satellite remote sensing, optical signal processing and display, etc. High-accuracy measurement of the polarization characteristics of light is essential, and a widely-used measurement method is to obtain the full-Stokes vector with a fully-automatic polarimetry (FAP), where rotating a quarter-waveplate and using the Fourier analysis are two key points. The FAP has obvious advantages in real-time detection and high measurement accuracy, which enables polarization parameters of light, such as the degree of polarization (DoP) and the angle of polarization (AoP), to be obtained efficiently. As for FAP, systematic analyses on its measurement errors are still crucial.

In this paper, we analyze the errors of FAP in terms of its three components: the quarter-waveplate, the linear polarizer and the photodiode. Firstly, the position error of the quarter-waveplate affects its fast-axis orientation, and the wavelength of light affects the retardance; secondly, the position error of the fixed polarizer disables it from the ideal vertical polarization orientation; thirdly, the intensity error of light measured by photodiode in FAP is sensitive to wavelength, and thus inevitably leads to a wavelength-dependent response. In fact, the position errors from quarter-waveplate and polarizer alter their Mueller matrices and thus finally influence the demodulation of the full-Stokes vector, while the errors from the photodiode affect the detected intensities used for Fourier analysis. In order to reduce above errors, we simulate the position errors of the quarter-waveplate and the polarizer to guide the installation of optical elements in FAP, which have great influences on demodulating the full-Stokes vector of light, we verify the feasibility of wavelength-based compensation for retardance error of quarter-waveplate, and we measure the wavelength response of the photodiode to compensate the photodiode's error.

Keywords: measurement error, fully-automatic polarimetry (FAP), polarization of light, waveplate, full-Stokes vector, position error

1. INTRODUCTION

Amplitude, frequency, phase and polarization are four basic and important parameters to describe the characteristics of light wave. Among them, the polarization property of light contains much unique information which is "visually blind" to human eyes [1-2]. When light wave interacts with substance, as usual, it will be reflected, transmitted and scattered, and the polarization state of light will experience some changes simultaneously. Note that such changes reflect the nature of substance itself which usually can't be reflected by the intensity of light wave [3-5]. Compared with analyzing the intensity information of light wave, analyzing and measuring the polarization state of light wave can provide more information of it and thus becomes greatly significant.

Polarization measurement technology has a wide range of applications in different fields. As the transmission speed increases in optical fiber communication, polarization mode dispersion (PMD) and polarization dependent loss (PDL) become technical barriers. The fundamental cause of PMD and PDL is the changes in the property of optical fiber itself, which then alters the polarization of light being transmitted in the fiber. Therefore, it is usually necessary to have a compensatory system to decrease PMD and PDL, and such a system depends on measuring the polarization state of light in real time and with high accuracy [6-7]. What's more, satellite remote sensing technology inverts characteristics of target through polarization information of the target, but it need to use reference light with known polarization to correct the

Twelfth International Conference on Information Optics and Photonics,
edited by Yue Yang, Proc. of SPIE Vol. 12057, 120574H
© 2021 SPIE · 0277-786X · doi: 10.1117/12.2606950

polarization remote sensor [8]. High-accuracy measurement of the polarization characteristics of light is essential, and a widely-used measurement method is to obtain the full-Stokes vector with a fully-automatic polarimetry (FAP), where rotating a quarter-waveplate and using the Fourier analysis are two key points [9]. Although polarization parameters of light, such as the degree of polarization (DoP) and the angle of polarization (AoP), can be efficiently obtained using FAP with the advantages of real-time and high accuracy, systematic analyses on the measurement errors of it are still crucial [10-12].

In this paper, firstly we introduce the measurement principle of FAP; then we analyze the errors of FAP from its three components: the quarter-waveplate, the linear polarizer and the photodiode; finally we simulate the influence of these errors to provide a guidance for the high-precision mounting of FAP or for error compensations through data treatments.

2. WORKING AND MEASUREMENT PRINCIPLE OF FAP

Nowadays, FAP is widely used to measure the polarization property of light because of its convenience and high efficiency [13-15]. Figure 1 shows the basic optical configuration of FAP, the transmission of optical light in it, and the working and measurement principle of it, where the incident light to be measured passes through the rotated quarter-waveplate driven by a stepper motor and a vertical polarizer, and the intensities of light modulated are obtained by detector.

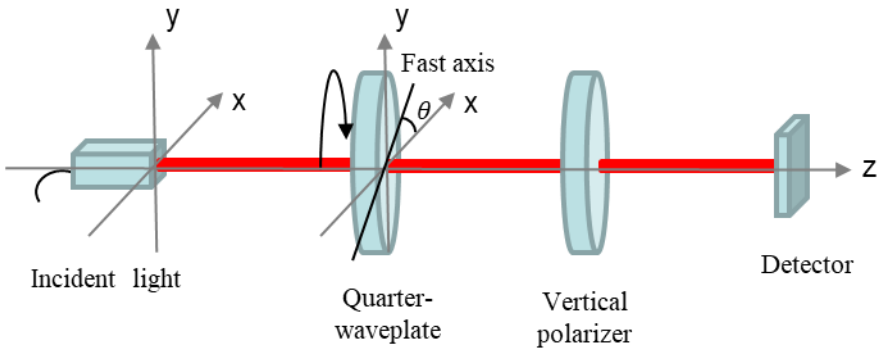

Figure 1. Schematic measurement principle of FAP.

Let's express the Stokes vector of the incident light by

$$S_{in} = \begin{bmatrix} S_0 \\ S_1 \\ S_2 \\ S_3 \end{bmatrix}, \tag{1}$$

where S_0 is the total intensity of light (*i.e.*, the intensity sum of 0° linearly-polarized and 90° linearly-polarized lights), S_1 is the intensity difference between 0° linearly-polarized and 90° linearly-polarized lights, S_2 is the intensity difference between 45° linearly-polarized and 135° linearly-polarized lights, and S_3 is the intensity difference between the right circularly-polarized and left circularly-polarized lights.

As shown in Fig. 1, let's select a right-hand coordinate system where the x-axis and y-axis are along the horizontal and vertical directions, respectively, and the incident light propagates along the z-axis. The Mueller matrix of the quarter-waveplate with its fast-axis at an angle θ to the x-axis can be written as

$$M(\theta) = \begin{bmatrix} 1 & 0 & 0 & 0 \\ 0 & cos^2 2\theta & sin2\theta cos2\theta & -sin2\theta \\ 0 & sin2\theta cos2\theta & cos^2 2\theta & cos2\theta \\ 0 & sin2\theta & -cos2\theta & 0 \end{bmatrix}, \tag{2}$$

and the Mueller matrix of vertical polarizer reads as

$$M_p = \frac{1}{2}\begin{bmatrix} 1 & -1 & 0 & 0 \\ -1 & 1 & 0 & 0 \\ 0 & 0 & 0 & 0 \\ 0 & 0 & 0 & 0 \end{bmatrix}. \tag{3}$$

Then the Stokes vector of the output light can be expressed by multiplying Eq. (3) and Eq. (2) and Eq. (1), as given by

$$S_{out} = M_p \cdot M(\theta) \cdot S_{in}. \tag{4}$$

The total intensity of output light $I(\theta)$, which is the first element of S_{out} in fact, can be expanded as

$$I(\theta) = \frac{1}{2}(S_0 - \frac{S_1}{2} + S_3 \sin 2\theta - \frac{S_2}{2}\sin 4\theta - \frac{S_1}{2}\cos 4\theta), \quad (5)$$

where θ is the rotation angle of fast-axis of quarter-waveplate to the x-axis. In this paper, the optical power is used to describe the intensity of light. For the quarter-waveplate driven by a stepper motor through N steps, $\theta = \omega t$, where ω is the angular frequency of the stepper motor's rotation. The Fourier series is usually used to analyze modulated intensities. According to Nyquist sampling theorem, the minimum sampling frequency should be twice the highest frequency of the signal. The sampling frequencies of S_1 and S_2 in time domain are $4\omega t$, so a minimum of 8 steps that make a complete rotation are required to perform the modulation. These coefficients are obtained by performing Fourier analysis on Eq. (5) and can be expressed by

$$A = S_0 - \frac{S_1}{2} = \frac{2}{N}\sum_{n=1}^{N} I(n\theta_j), \quad (6)$$

$$B = S_3 = \frac{4}{N}\sum_{n=1}^{N} I(n\theta_j) sin2n\theta_j, \quad (7)$$

$$C = -\frac{S_2}{2} = \frac{4}{N}\sum_{n=1}^{N} I(n\theta_j) sin4n\theta_j, \quad (8)$$

$$D = -\frac{S_1}{2} = \frac{4}{N}\sum_{n=1}^{N} I(n\theta_j) cos4n\theta_j, \quad (9)$$

where the step of motor $\theta_j = \frac{2\pi}{N}$. By solving Eqs. (6)-(9), the Stokes vector elements of the incident light are calculated by

$$S_0 = A - D, \quad (10)$$

$$S_1 = -2D, \quad (11)$$

$$S_2 = -2C, \quad (12)$$

$$S_3 = B. \quad (13)$$

The AoP and the DoP of the incident light can then be respectively calculated by

$$AoP = \frac{1}{2} arctan \frac{S_2}{S_1}, \quad (14)$$

$$DoP = \frac{\sqrt{S_1^2 + S_2^2 + S_3^2}}{S_0}. \quad (15)$$

3. ERROR ANALYSIS

To enhance the accuracy of FAP, systematic analyses on the measurement errors of it are crucial [16-17]. We analyze the errors of FAP from its three components: the quarter-waveplate, the linear polarizer and the photodiode used as the detector. Firstly, we analyze the influence of the wavelength of light and the position error of the quarter-waveplate that affects its fast-axis orientation; secondly, we analyze the position error of the fixed polarizer that disables it from the ideal vertical polarization orientation; thirdly, we analyze the intensity error of light measured by the photodiode in FAP that is sensitive to wavelength, which inevitably leads to a wavelength-dependent response. The errors of quarter-waveplate is discussed in Section 3.1; the polarizer error is discussed in Section 3.2; and the error of photodiode is discussed in Section 3.3.

3.1 Errors of quarter-waveplate

There are two factors that affect the Mueller matrix of the quarter-waveplate, which are the retardance and the position of fast-axis.

3.1.1 Retardance error of quarter-waveplate

Although FAP uses achromatic quarter-waveplates, the retardance error ε_1 related to the wavelength describe the retardance difference from the ideal value of $\frac{\pi}{2}$. When a beam of light is incident perpendicularly upon the surface of a wave-plate, it is decomposed into the ordinary and the extraordinary rays whose vibrational directions are vertical to each other, and the corresponding refractive indexes are n_o and n_e [18-20]. The correlation between the retardance and the wavelength is given by

$$\delta = \frac{2\pi(n_e - n_o)d}{\lambda}, \quad (16)$$

where δ is the retardance of the quarter-waveplate, λ represents the wavelength of the incident light, and d represents the thickness of the waveplate.

Note that different wavelength corresponds to different retardance of the quarter-waveplate, which alters the Mueller matrix to

$$M(\delta,\theta)=\begin{bmatrix}1 & 0 & 0 & 0\\ 0 & cos^2 2\theta+sin^2 2\theta cos\delta & (1-cos\delta)sin2\theta cos2\theta & -sin2\theta sin\delta\\ 0 & (1-cos\delta)sin\theta cos2\theta & sin^2 2\theta+cos^2 2\theta cos\delta & cos2\theta sin\delta\\ 0 & sin2\theta sin\delta & -cos2\theta sin\delta & cos\delta\end{bmatrix}, \quad (17)$$

where the retardance $\delta=\frac{\pi}{2}+\varepsilon_1$. By replacing $M(\theta)$ in Eq. (4) by $M(\delta,\theta)$, the output intensity becomes

$$I(\delta,\theta)=\frac{1}{2}[S_0-\frac{S_1}{2}(1+cos\delta)+S_3 sin\delta\, sin\,2\theta-\frac{S_2}{2}(1-cos\delta)sin4\theta-\frac{S_1}{2}(1-cos\delta)cos4\theta)]. \quad (18)$$

Similarly, adopting the demodulation process as shown in Section 2, the four parameters of the Stokes vector of the incident light are rewritten as

$$S_0=A-\frac{1+cos\delta}{1-cos\delta}D, \quad (19)$$

$$S_1=\frac{-2D}{1-cos\delta}, \quad (20)$$

$$S_2=\frac{-2C}{1-cos\delta}, \quad (21)$$

$$S_3=\frac{B}{sin\delta}. \quad (22)$$

For simulation, let us set the retardance error ε_1 between $-\frac{\pi}{5}$ and $\frac{\pi}{5}$, the four parameters of the Stokes vector of the incident light as 50mW, 25mW, $25\sqrt{3}$mW, and 0mW, respectively, and the AoP and DoP of incident light as 30° and 1. The simulation results calculated by Eqs. (19)-(22) and Eqs. (14)-(15) are shown in Fig. 2 and Fig. 3.

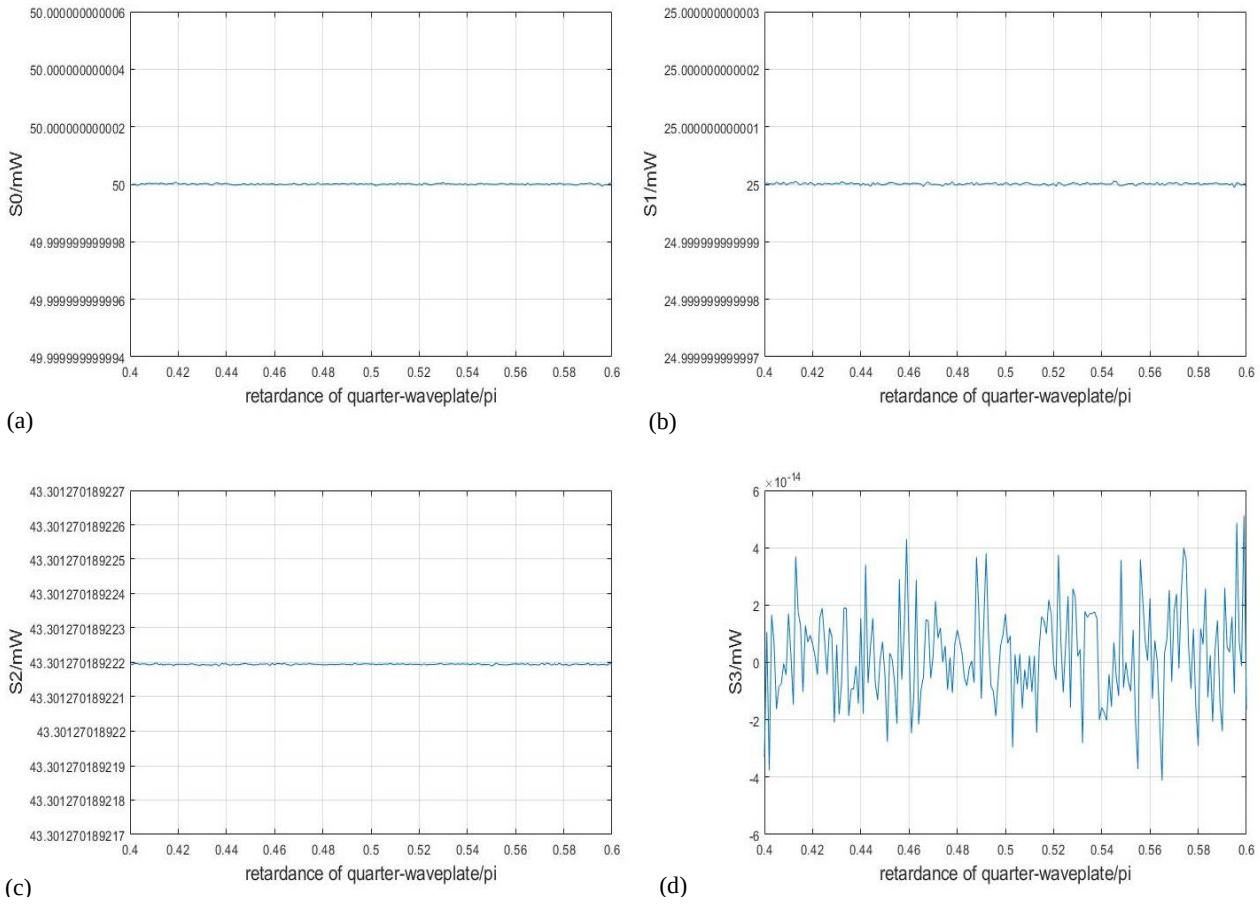

Figure 2. Calculated parameters of the Stokes vector of the incident light (a) S_0; (b) S_1; (c) S_2 and (d) S_3 where retardance δ changes from $\frac{2\pi}{5}$ to $\frac{3\pi}{5}$.

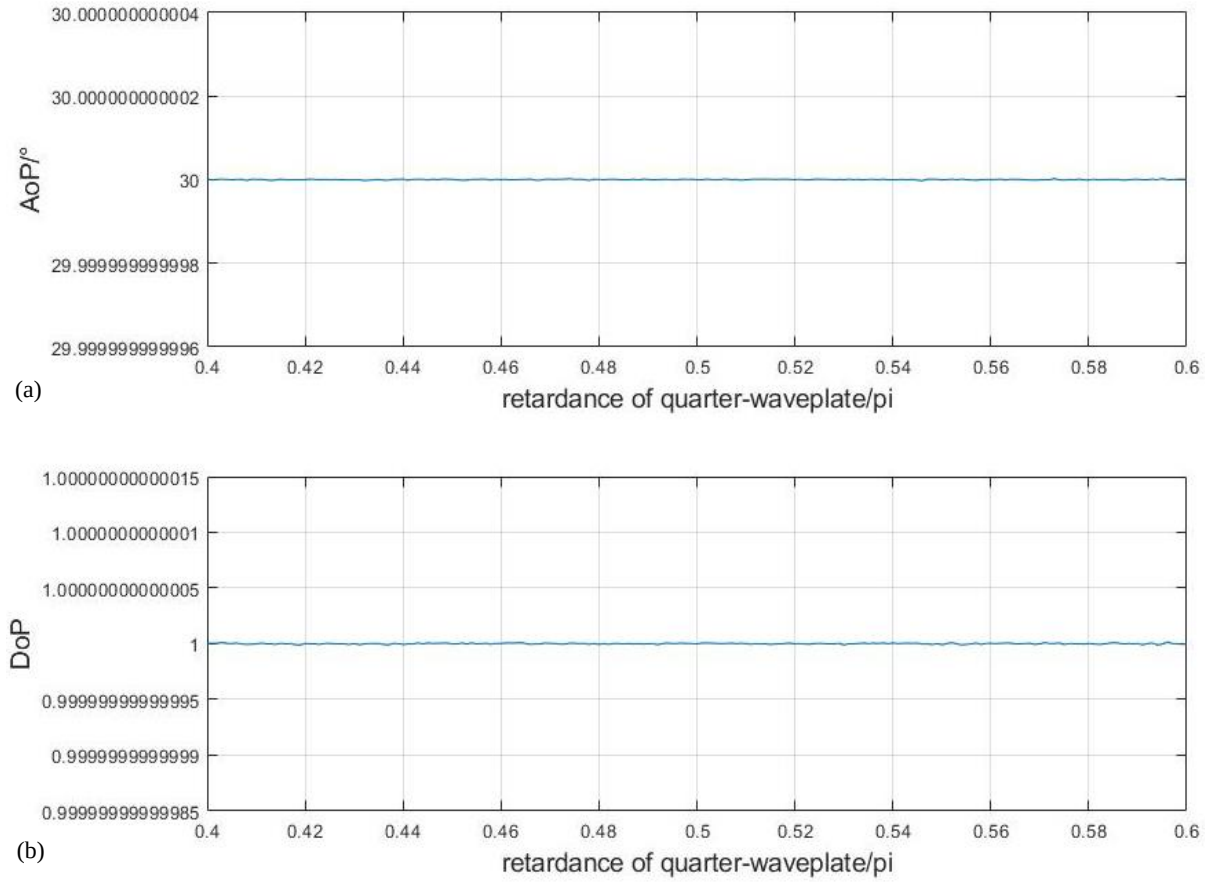

Figure 3. Calculated polarization parameters of the incident light when retardance δ changes from $\frac{2\pi}{5}$ to $\frac{3\pi}{5}$. (a) for AoP and (b) for DoP.

From Fig. 2 and Fig. 3, we observe that the calculated parameters of the Stokes vector (S_0, S_1, S_2 and S_3) and the polarization parameters (AoP and DoP) of the incident light are close to the ones we set, meaning that Eqs. (19)-(22) can well compensate the retardance error related to the wavelength.

3.1.2 Position error of quarter-waveplate

Another influence factor of the quarter waveplate is its fast-axis's position error ε_2, it describes the fast-axis orientation difference between the real angle (denoted by θ') and the ideal angle (denoted by θ). This is owing to the fact that there always exists a mechanical error when rotating the quarter-waveplate by a stepper motor, which can be expressed by

$$\theta' = \theta + \varepsilon_2. \tag{23}$$

In this case, the Mueller matrix of the quarter-waveplate turns into

$$M(\tfrac{\pi}{2}, \theta') = \begin{bmatrix} 1 & 0 & 0 & 0 \\ 0 & cos^2 2\theta' & sin2\theta' cos2\theta' & -sin2\theta' \\ 0 & sin2\theta' cos2\theta' & sin^2 2\theta' & cos2\theta' \\ 0 & sin2\theta' & -cos2\theta' & 0 \end{bmatrix}, \tag{24}$$

and then the output intensity can be rewritten by

$$\begin{aligned} I(\varepsilon_2, \theta) = \tfrac{1}{2}[S_0 - \tfrac{S_1}{2} + S_3 cos2\varepsilon_2 \, sin\, 2\theta + S_3 sin2\varepsilon_2 \, cos\, 2\theta \\ + \tfrac{1}{2}(S_1 sin4\varepsilon_2 - S_2 cos4\varepsilon_2) sin\, 4\theta - \tfrac{1}{2}(S_1 cos4\varepsilon_2 + S_2 sin4\varepsilon_2) cos\, 4\theta]. \end{aligned} \tag{25}$$

It's easy to verify that Eq. (25) becomes to Eq. (5) when $\varepsilon_2 = 0$.

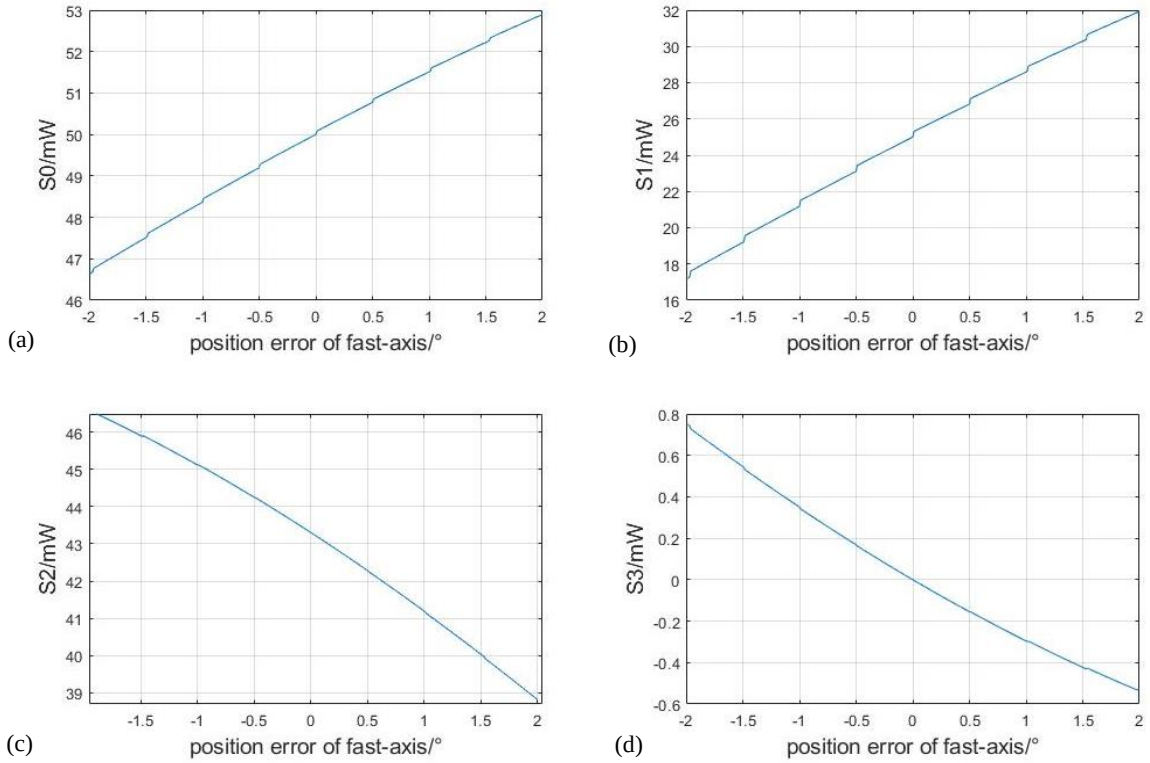

Figure 4. Calculated parameters of the Stokes vector of the incident light (a) S_0; (b) S_1; (c) S_2 and (d) S_3 where the position error of fast-axis of the quarter-waveplate ε_2 changes from -2° to 2°.

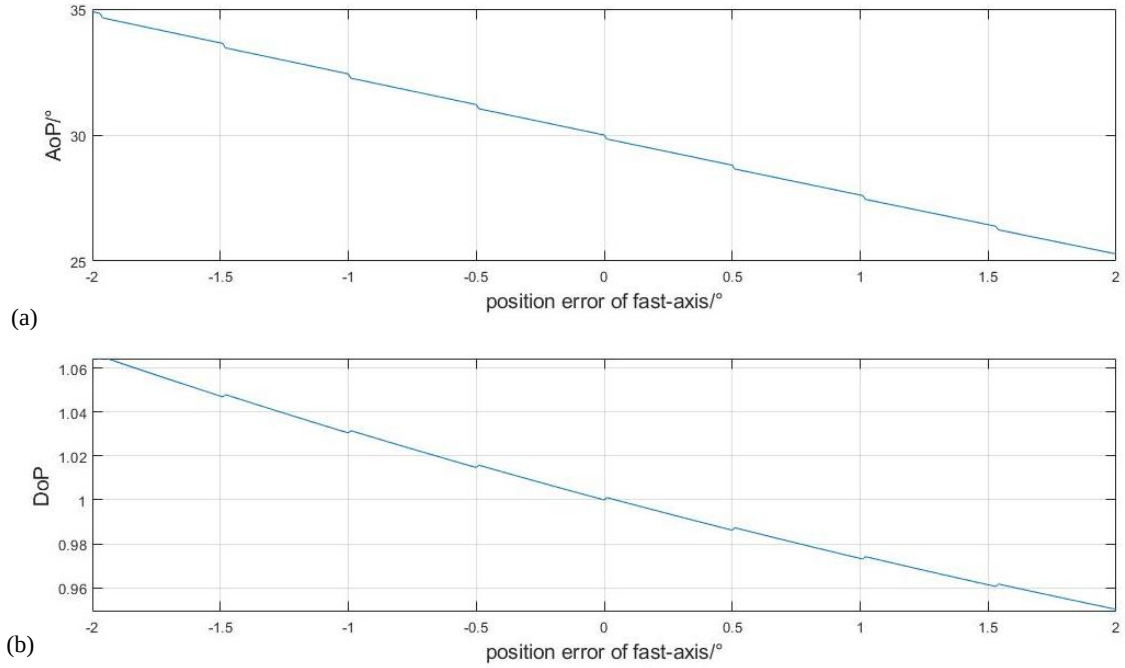

Figure 5. Calculated polarization parameters of the incident light when position error of fast-axis ε_2 changes from $-2°$ and 2°. (a) for AoP and (b) for DoP.

For the simulation, let us set the position error ε_2 between -2° and 2°, and other parameters of the incident light are the same as that chosen in Section 3.1.1. By replacing $I(n\theta_j)$ in Eqs. (6)-(9) with $I(\varepsilon_2, n\theta_j)$ expressed by Eq. (25) where $\theta = n\theta_j$, we calculate the parameters of the Stokes vector (S_0, S_1, S_2 and S_3) and the polarization parameters (AoP and DoP) of the incident light by using Eqs. (10)-(15). The corresponding simulation results are shown in Fig. 4 and Fig. 5, respectively.

The variation of the computed parameters of Stokes vector with the position error of fast-axis is shown in Fig. 4, and corresponding variation of the computed polarization parameters (AoP and DoP) is shown in Fig. 5. It is clearly seen that, with the increase of the position error of the fast-axis, the departures of both the AoP and the DoP from their actual values we set (30° and 1, respectively) increase. Figure 4 and Figure 5 also show that, when there is no position error of the fast axis, *i.e.*, ε_2=0°, the computed value of every parameter is just the same as that we set. As far as the measurement application is concerned, to ensure both AoP and DoP measurement accuracies of FAP less than 1%, we must keep the position error ε_2 in the range of -0.14° and 0.08°, as shown in Fig. 5.

3.2 Error of vertical polarizer

The vertical polarizer is fixed in the system of FAP, but there exists a position error ε_3 that prevents it from being vertical in the installation process. The actual position angle φ is written as

$$\varphi = \frac{\pi}{2} + \varepsilon_3. \tag{26}$$

Then the Mueller matrix of polarizer changes into

$$M_P(\varphi) = \frac{1}{2}\begin{bmatrix} 1 & cos2\varphi & sin2\varphi & 0 \\ cos2\varphi & cos^2 2\varphi & sin2\varphi cos2\varphi & 0 \\ sin2\varphi & sin2\varphi cos2\varphi & sin^2 2\varphi & 0 \\ 0 & 0 & 0 & 0 \end{bmatrix}. \tag{27}$$

As the Mueller matrix alters, the output intensity goes to

$$\begin{aligned} I(\varphi,\theta) = \frac{1}{2}[S_0 + \frac{S_1}{2}cos2\varphi + \frac{S_2}{2}sin2\varphi - S_3 cos2\varphi\, sin\,2\theta + S_3 sin2\varphi\, cos\,2\theta \\ + \frac{1}{2}(S_1 sin2\varphi + S_2 cos2\varphi)sin\,4\theta + \frac{1}{2}(S_1 cos2\varphi - S_2 sin2\varphi)cos\,4\theta]. \end{aligned} \tag{28}$$

Similarly, using Eq. (28) to calculate the output intensity of light and replacing $I(n\theta_j)$ in Eqs. (6)-(9) with $I(\varphi, n\theta_j)$, expressed by Eq. (28) where $\theta = n\theta_j$, again we calculate the parameters of the Stokes vector (S_0, S_1, S_2 and S_3) and the polarization parameters (AoP and DoP) of the incident light by using Eqs. (10)-(15). For the simulation, let us set the position error of the vertical polarizer ε_3 between -2° and 2°, and other parameters of the incident light are the same as that chosen in Section 3.1.1. The corresponding simulation results are shown in Fig. 6 and Fig. 7, respectively.

From Fig. 6 and Fig. 7, we can find a linear variation of S_0, S_1 and S_2 except S_3. What's more, with the departure increase of the position angle of polarizer, the difference between the calculated AoP of the incident light and the ideal one we set increases accordingly. Such a variation feature is also the same for the DoP. These mean that the polarization measurement error of FAP increases. Figure 7 indicates that, to achieve a measurement error less than 1% for both the AoP and the DoP, it is necessary to keep the position error of the vertical polarizer within -0.3° and 0.3°.

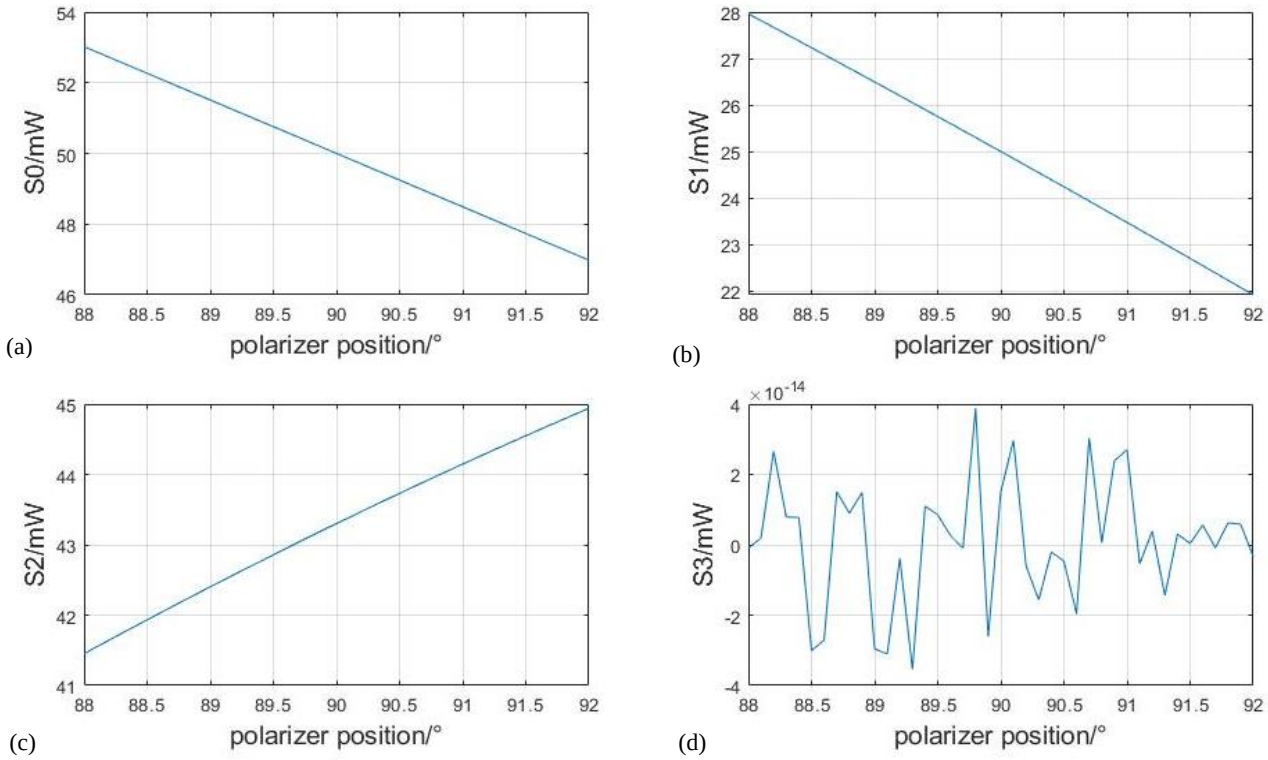

Figure 6. Calculated parameters of the Stokes vector of the incident light (a) S_0; (b) S_1; (c) S_2 and (d) S_3 where the position angle of the polarizer φ changes from 88° to 92°.

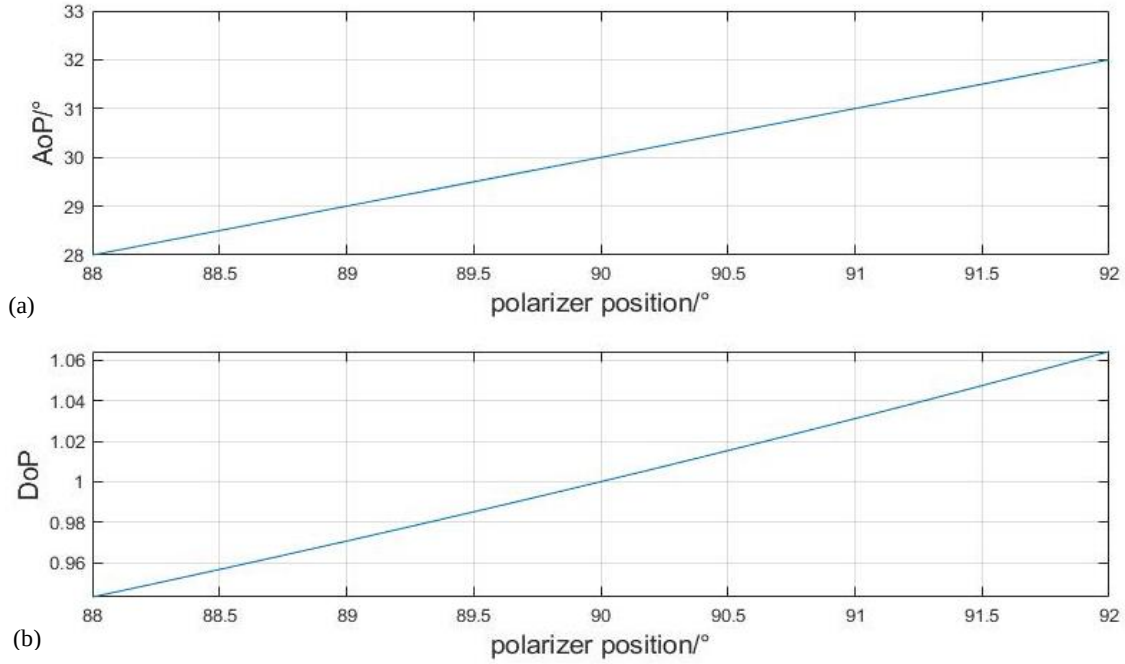

Figure 7. Calculated polarization parameters of the incident light when position angle of the polarizer φ changes from 88° to 92°. (a) for AoP and (b) for DoP.

3.3 Error of photodiode

As usual, a PIN photodiode is used to detect the intensity modulated by quarter-waveplate and vertical polarizer, and the PIN photodiode is a photoelectric conversion device that converts a received light signal into an electrical signal output [21-23]. However, the output electrical signal of photodiode is related not only to the light intensity, but also to the wavelength of the incident light. Light with same intensity but different wavelength produces different response, the errors from the photodiode affect the detected intensities used for Fourier analysis. To reduce the intensity error caused by the wavelength on the photodiode, investigating its spectral responsivity is necessary.

Spectral responsivity characterizes the sensitivity of the photosensitive element. For an optical power radiation at wavelength λ of light, the relationship between the electrical signal and the optical signal can be expressed as:

$$R_I(\lambda) = \frac{I(\lambda)}{P(\lambda)}, \tag{29}$$

where $R_I(\lambda)$ is spectral responsivity at wavelength λ, $P(\lambda)$ represents optical power of incident light at wavelength λ, $I(\lambda)$ is the output signal current of the photodiode with the incident optical power. We can use the spectral responsivity of the photodiode to compensate the photodiode's error.

4. CONCLUSION

To improve the measurement accuracy of FAP, the analysis on its measurement errors is necessary. We analyze the errors of FAP from its three components: the quarter-waveplate, the linear polarizer and the photodiode. The factors causing measurement error in FAP are as follows, the retardance error of the quarter-waveplate based on wavelength, the position errors of the quarter-waveplate's fast-axis and the vertical polarizer, and the intensity error of the photodiode.

Our analyses indicate that the retardance error of the quarter-waveplate should be compensated with wavelength, and the intensity error of photodiode should be corrected by spectral responsivity. Simulation indicates that, in order to ensure the AoP and DoP measurement accuracies of FAP less than 1%, we require to control the position error of quarter-waveplate's fast-axis within -0.14° and 0.08°, the position error of the vertical polarizer within -0.3° and 0.3°. Our research work also indicates that, by systematically comparing the measured polarization parameters with the known ones for each given input light, and on the basis of their differences (including the magnitude, the positive/negative sign and even the variation tendency), we actually can improve the polarization measurement accuracy of the FAP either by assisting its elements installation to reduce the assemble errors or by optimizing the data treatment to make a compensation.

ACKNOWLEDGMENTS

This work was supported by Natural Science Foundation of Shaanxi Province (2021JM-204); Xi'an Scientific and Technological Projects (2020KJRC0013); Postgraduate Innovation Team Project of Shaanxi Normal University (TD2020030Y).

REFERENCES

[1] H. Berry, G. Gabrielse, and A. Livingston, "Measurement of the Stokes parameters of light," Applied Optics. 16(12), 3200-3205 (1977).
[2] M. Yamanari, Y. Yasuno, S. Makita, Y. Nakamura, Y. Hori, M. Itoh, and T. Yatagai, "Polarization sensitive Fourier domain optical coherence tomography with continuous polarization modulation," SPIE BiOS. 6079, 415-420 (2006).
[3] W. Groner, J. W. Winkelman, A. G. Harris, C. Ince, G. J. Bouma, K. Messmer, and R. G. Nadeau, "Orthogonal polarization spectral imaging: A new method for study of the microcirculation," Nature Medicine. 5(10), 1209-1212 (1999).
[4] J. Greiner, S. Klose, K. Reinsch, H. M Schmid, R. Sari, D. H Hartmann, C. Kouveliotou, A. Rau, E. Palazzi, and C. Straubmeier, "Evolution of the polarization of the optical afterglow of the γ-ray burst GRB030329," Nature. 426(9), 157-159 (2003).
[5] H. Takasaki, "Automatic polarimetry by means of an ADP polarization modulator," Applied Optics. 35(5), 759764 (1996).

[6] F. Buchali, H. Bulow, "Adaptive PMD compensation by electrical and optical techniques," Journal of Lightwave Technology. 22(4), 1116-1126 (2004).
[7] A. Eyal, D. Kuperman, O. Dimenstein, and M. Tur, "Polarization dependence of the Intensity modulation transfer function of an optical system with PMD and PDL," IEEE Photonics Technology Letters. 14(11), 1515-1517 (2002).
[8] J. Abraham, Franklin, L. J. Otten, D. Meigs, R. D. Sears, T. Turner, and J. Hair, "Measurements of backgrounds and target object polarization using visible-band hyperspectral imagery," SPIE. 3375, 328-324 (1998).
[9] D. H. Goldstein, [Polarized Light, Third Edition], CRC Press, Huntsville, 31-55 (2010).
[10] L. Li, Y. Li, Q. Chi, K. Liu, X. B. Zhang, and J. H. Li, "Optimized imaging polarimeter for measuring polarization properties of hyper number aperture lithography tools," SPIE. 9282, 928232 (2014).
[11] M. J. Duggin, "Imaging polarimetry in scene element discrimination," Proceedings of SPIE. 3754, 108-117 (1999).
[12] D. Goldstein, R. Chipman, "Error analysis of a Mueller matrix polarimeter," Journal of the Optical Society of America A. 7(4), 693-700 (1990).
[13] R. M. Azzam, "Photopolarimetric measurement of the Mueller matrix by Fourier analysis of a single detected signal," Optics Letters. 2(6), 148-150 (1989).
[14] D. Aspnes, P. Hauge, "Rotating- compensator/analyzer fixed- analyzer ellipsometer: Analysis and comparison to other automatic ellipsometers," Journal of the Optical Society of America. 66(9), 949-954 (1976).
[15] L. Chen, J. Hong, Y. Qiao, X. Sun, and Y. Wang, "Accuracy analysis on a sort of polarized measurement in remote sensing," Spectroscopy and Spectral Analysis, 28(10), 2384-2387 (2008).
[16] K. Ichimoto, B. Lites, D. Elmore, Y. Suematsu, S. Tsuneta, Y. Katsukawa, T. Shimizu, R. Shine, T. Tarbell, and A. Title, "Polarization calibration of the solar optical telescope onboard Hinode," Solar Physics. 249, 233–261 (2008).
[17] E. Dijkstra, H. Meekes, and M. Kremers, "The high-accuracy universal polarimeter," Journal of Physics D. 24, 1861–1868 (1991).
[18] D. H. Goldstein, "Mueller matrix dual-rotating retarder polarimeter," Applied Optics. 31, 6676–6683 (1992).
[19] P. Williams, A. H. Rose, and C. Wang, "Rotating-polarizer polarimeter for accurate retardance measurement," Applied Optics. 36(25), 6466-6472 (1997).
[20] X. Zhang, F. Wu, and H. Wang, "Simultaneous measurement of phase retardation and optic axis of wave plates," Optoelectronics Letters. 3(1), 65-68 (2007).
[21] Y. Cui, H. Wang, and L. Zhang, "Measurement of the spectral responsivity of silicon photodiodes," Physical Experiment of College. 18(3), 61-63 (2005).
[22] S. Tomczyk, R. Casini, A. G. De Wijn, and P. G. Nelson, "Wavelength diverse polarization modulators for stokes polarimetry," Applied Optics. 49, 3580–3586 (2010).
[23] Y. Liang, Z. Qu, Y. Zhong, Z. Song, and S. Li, "Analysis of errors in polarimetry using a rotating waveplate," Applied Optics. 58(36), 9883-9895 (2019).